# Iterative Space Time Block Equalizer for Single Carrier Systems with Receiver Nonlinearity

Talha Faizur Rahman, Vuk Marojevic
Department of Electrical and Computer Engineering
Mississippi State University - MS
Email: {tfr42, vuk.marojevic}@msstate.edu

Abstract—Receiver nonlinearity gives rise to intermodulation products that are caused by two strong adjacent channel signals called blockers. The nonlinear distortion effects are significantly higher for multiple antenna wideband systems in dispersive environments because third order intermodulation products decreases the signal-to-noise ratio (SNR) at the output of the equalization process. This complicates the demodulation process and increases the bit error rate. This paper considers such nonlinear distortion in the context of space-time shift keying (STSK)-enabled wideband single-carrier systems and proposes an iterative space-time block equalization (ISTBE) framework for frequency domain equalization. We present our design of a practical ISTBE receiver based on the turbo principle and numerically demonstrate that it effectively removes the residual inter-symbol interference while suppressing high-power blockers and the in-band intermodulation distortion that they cause. The proposed system is thus suitable for simple wideband radio frequency front ends operating in the weak nonlinear region and enables adjacent channel spectrum coexistence with heterogeneous transmitters and receivers of different qualities.

Index Terms—Single-carrier, STSK, receiver nonlinearity, iterative equalization.

### I. INTRODUCTION

Recent times have seen unprecedented demand for wireless services and this demand is expected to further increase with the introduction of sophisticated beyond 5G (B5G) services [1]. Consequently, radio frequency (RF) spectrum, which is an expensive commodity, will need to accommodate an increasing number of connected devices. With this background, researchers as well as regulators are exploring new ways for seamless coexistence of heterogeneous radios in shared spectrum to improve spectrum utilization [2]. Enabling technologies such as cognitive radio empowered by software radios, massive multiple-input, multiple-output (MIMO) antenna systems, and millimeter wave radios, are being put in practice to efficiently use and share spectrum without degrading the wireless services. For instance, cognitive radiobased Internet of Things (IoT) is considered in [3] to increase the resource allocation with minimum energy consumption. Massive MIMO-based IoT is proposed to support massive connectivity [4]. But massive connectivity in congested radio environments poses threats to receivers where adjacent channel blockers can cause distortion in the desired channels due to RF front end nonlinearity of practical receivers. This is illustrated in Fig. 1 and affects the radio communications performance, requiring compensation at the receiver.

MIMO-based systems not only support massive connectivity in adverse environments, but also help against hardware nonlinearity through diversity. The resiliency against channel and hardware impairments can be enhanced with sophisticated receiver designs [5]. Recently, space-time MIMO techniques have gained traction as a result of their versatility for provisioning good performance in urban environments. But unlike spatial modulation and spatial multiplexing, a MIMO-variant called space-time shift keying (STSK) [6] provides the much needed flexibility and tradeoff between diversity and multiplexing through parameterization that is independent of the underlying hardware. This has been proven for narrowband channels.

For wideband single-carrier systems, the receiver needs to be carefully designed to leverage the STSK diversity gains [7]. We therefore introduce and analyze the performance of an iterative space-time block equalizer (ISTBE) for STSK-aided single-carrier frequency domain equalization (SC-FDE) in the presence of receiver nonlinearity. The proposed ISTBE efficiently exploits the diversity and neutralizes the effects of RF nonlinearity without the need for separate compensation. This paper provides the following contributions:

- We design an efficient ISTBE based on the turbo principle for STSK-aided SC-FDE (SSF);
- We demonstrate that the frequency agile SSF-ISTBE framework is robust against receiver nonlinearity in the presence of strong adjacent channel blockers, as opposed to its minimum mean square error (MMSE) counterpart;
- We derive the computational complexity of the SSF-ISTBE and show that it is only slightly higher than that of the SSF-MMSE receiver.

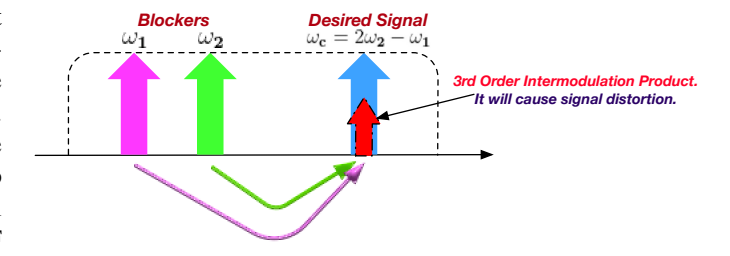


Fig. 1. Adjacent channel interference causing co-channel signal distortion due to the 3rd order intermodulation product.

The rest of the paper is structured as follows: Section II discusses the related work and Section III defines the system model. Section IV introduces the ISTBE framework. Section V provides the details about the simulation setup and presents the results. The conclusions are drawn in Section VI.

### II. RELATED WORK

STSK-based systems, such as STSK-orthogonal division frequency multiplexing (OFDM) [6], allows employing maximum likelihood receivers because individual subcarriers are narrowband and, thus, experience flat fading. However, the performance is significantly compromised in frequency selective wideband channels. This has been shown in [7], where STSK-aided single-carrier FDMA (SC-FDMA) is proposed for dispersive channels. Note that the performance gains of general MIMO-OFDM systems with sub-optimal MMSE receivers vanish in dispersive fading channels.

Iterative space-time equalization for single carrier systems is proposed in [5] which presents a design and performance analysis with ideal and practical power amplifiers at the transmitter. The iterative receiver does not only minimize the non-linear power amplifier distortion, but also outperforms STSK-OFDM systems in highly dispersive channel conditions. The frequency domain version of the turbo equalizer for single-carrier spatial modulation (SM) is considered in [8] and the time-domain version is considered in [9], enabling soft-decision feedback for canceling the residual interference. The authors of [10] use the linear approach proposed in [7] for SSF systems in millimeter wave channels. They show that the SSF receiver with a linear MMSE outperforms the SM-aided SC-FDE in the presence of hardware impairments and channel estimation errors.

Radio transmitters and receivers are nonlinear and with the emergence of IoT, transceivers of different quality and signal power levels will need to coexist. Spectrum sensing in the presence of receiver nonlinearity is considered in [11], which proposes a scheme for canceling the intermodulation product. Receiver nonlinearity can cause a 5 dB SNR loss with strong adjacent channel blockers in shared spectrum [12]. This is important to consider for receivers with wideband preselection filters and nonlinear RF front ends.

### III. SYSTEM MODEL

We first provide the model for capturing the nonlinear behavior of receivers. We then introduce the SSF framework.

### A. Receiver Nonlinearity

Adjacent channel signals entering a nonlinear receiver generate intermodulation products, which can be modeled using the polynomial approximation for wideband signals as [12],

$$y(t) = \alpha_1 s(t) + \alpha_2 [s(t)]^2 + \alpha_3 [s(t)]^3 + \cdots$$
 (1)

Parameters  $s\left(t\right)$  and  $y\left(t\right)$  are the received signal at the input and output of the nonlinear RF front end. Parameter  $\alpha_{i}$  corresponds to the  $i^{th}$  order gain. The first term is the desired signal with a linear gain. The third, fifth, and higher order

terms may fall in the band of interest, with the third order term being the strongest. We consider the presence of the desired signal at  $\omega_c$  which is adjacent to the angular frequencies  $\omega_1$  and  $\omega_2$  where strong blocker signals are present, such that  $2\omega_1-\omega_2=\omega_c$  or  $2\omega_2-\omega_1=\omega_c$ . Such blockers can cause third order intermodulation distortion at  $\omega_c$ , as illustrated in Fig. 1.

The baseband representation of a wideband signal at the output of nonlinear receiver can be approximated as [13],

$$y(t) = \alpha_1 s(t) + \frac{3}{2} \alpha_3 b(t)^2 c^*(t) + z(t),$$
 (2)

where b(t) and c(t) are the blocker signals at  $\omega_1$  and  $\omega_2$ , respectively, and z(t) is the additive white Gaussian noise (AWGN) in the band of interest. It is worth mentioning that the input amplitude corresponding to the third-order intercept point  $IP_3$  is related to  $\alpha_1$  and  $\alpha_3$  as [11],

$$A_{IP_3} = \sqrt{\frac{4}{3} \frac{\alpha_1}{\alpha_3}}. (3)$$

The input power in dBm at the third order intercept point can be obtained as [12],

$$P_{IP_3} = 20 \log_{10} A_{IP_3} + 10 [dBm].$$
 (4)

The  $\mathrm{IP}_3=(\mathrm{IIP}_3,\mathrm{OIP}_3)$  is an important property of nonlinear RF components. It defines the input power for which the output power of the extrapolated fundamental signal term equals that of the extrapolated cubic term, being the result of the third order intermodulation of two strong signals that enter a nonlinear device. Fig. 2 illustrates this. It represents the result from the two-tone test applied to a nonlinear device.

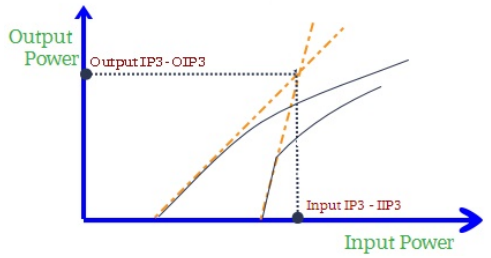


Fig. 2. Illustration of the third order intercept point - IP<sub>3</sub>.

### B. The SSF Framework

We consider a single-carrier block transmission with cyclic prefix (CP) and multiple antennas at the transmitter and at the receiver. The transceiver is employing STSK with M transmit and N receive antennas. We assume that the cardinality Q of the dispersion matrix (DM) is available at the transceiver. The transmitter architecture, which is shown in Fig. 3, divides the input bit stream into two bit stream subsets, one for indexing the q-th dispersion matrix,  $A_q$ , and the other for the modulation mapping, s. It is important to note that the dispersion matrix set  $A_q$  is derived offline for the modulation order of the underlying phase shift keying (PSK) or quadrature amplitude modulation (QAM) and that it is available at the receiver for coherent demodulation.

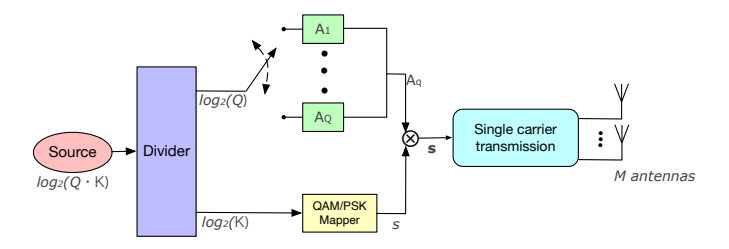


Fig. 3. STSK-aided single-carrier transmitter.

The generated STSK codeword is stored in a buffer of  $N_F$  symbols that is kept equal to the size of the frequency domain equalizer block at the receiver. The transmission block is passed through pulse shaping filters before being transmitted from M antenna elements.

The STSK codeword s is generated with  $log_2(Q)$  bits indexing the q-th DM among the Q available DMs, each of size  $M \times T$ , where T is the duration of the STSK-codeword. The selected DM disperses the energy of the k-th input information symbol, taken from a K-ary PSK or QAM constellation. The STSK-codeword is then given as,

$$\mathbf{s}_n = 0 \cdot s_k A_1 + \dots + 1 \cdot s_k A_q + \dots + 0 \cdot s_k A_Q, \quad (5)$$

where  $\mathbf{s}_n \in \mathbb{C}^{M \times T}$ . STSK is based on the index modulation principle in which only a single DM is activated at any given time during the n-th symbol period in a block. Every column of the selected matrix is then transmitted from the M-antenna array at a baud-rate of  $T/T_{N_F}$ , where  $T_{N_F}$  is the time duration of the transmitted block. The desired signal power is P, whereas the signal powers of blockers b and c are B and C.

Specific STSK configurations are identified as (M, N, T, Q), where N is the number of receive antennas and T accounts for the degree of time diversity provided that  $M \geq T$ . The DM sets are generated in advance and made available to the SC-FDE system prior to transmission. The matrices are generated using the optimization rule of [6].

At the receiver, the signal passes through a wideband channel selection filter followed by non-linear amplifier. This allows frequency agility and reduces cost. WiFi receivers typically have wideband front end filters. Software radios may or may not employ filtering in the analog domain to be tunable to a wide range of frequencies. This allows for adjacent channel blockers to enter the receiver unattenuated, which may cause operation in the weak nonlinearity region—considered here—or strong nonlinear distortion, such as clipping at the analog-to-digital converter. The low noise amplifier (LNA) is inherently nonlinear and two or more strong signals that drive it into nonlinear operation will combine and generate intermodulation products.

We assume two blockers that appear at frequencies such that the third order intermodulation product falls into the band of the signal of interest as illustrated in Fig. 1. Without loss of generality, blockers are modulated and pulse shaped single-carrier signals of single-input, singe-output systems. The receiver of interest has no information about them.

For notation simplicity we drop the time index from (2). The signal representation at the output of the LNA then becomes,

$$\mathbf{y} = \alpha_1 \mathbf{h} \mathbf{s} + \xi + \mathbf{z},\tag{6}$$

where,

$$\xi = \frac{3}{2}\alpha_3 \mathbf{b}^2 \mathbf{c}^*,\tag{7}$$

is the nonlinear distortion term in the band of the signal of interest,  $\mathbf{h}$  is the channel matrix of size  $N \times M$ ,  $\mathbf{z}$  is the  $N \times T$  AWGN matrix of i.i.d. components with zero mean and  $\sigma_0^2$  variance, and  $\mathbf{s} = [\mathbf{s}_1, \cdots, \mathbf{s}_{N_F}]$  is the block of  $N_F$  transmitted STSK codewords of size  $M \times T$  each.

## IV. PROPOSED ITERATIVE DECODING OF THE SSF IN THE PRESENCE OF RECEIVER NONLINEARITY

In this section, we introduce the proposed ISTBE framework by developing the mathematical derivations of the feed forward (FF) and the feedback (FB) filter coefficients.

Unlike multi-carrier/OFDM systems, SC-FDE does not employ the inverse FFT (IFFT) at the transmitter and, therefore, sub-optimal equalization in the frequency domain is the only viable solution to decode the signal [10]. However, the SC-FDE multi-user variant, called SC-FDMA, does employ the discrete Fourier transform (DFT) as well as the IFFT for multi-user transmission [14]. The performance of sub-optimal linear approaches, such as the MMSE and zero forcing, may be far from the matched filter bound [5]. This is due to the inability of linear equalizers to remove the existing inter-symbol interference (ISI) at the output of the equalization process. In order to tackle this issue, we propose a nonlinear frequency domain iterative decoding technique that is specifically designed for SSF systems.

Fig. 4 illustrates the ISTBE. The distorted signal y is converted from analog to digital, followed by the CP removal and frequency domain equalization. The frequency domain estimated block after the i-th equalization iteration is,

$$\bar{\mathbf{S}}_i = \mathbf{F}_i \mathbf{Y} - \mathbf{B}_i \hat{\mathbf{S}}_{i-1}, \tag{8}$$

where  $\mathbf{F}_i$  is an  $M \times N$  matrix containing the FF coefficients for the SSF block,  $\mathbf{B}_i$  is the  $M \times M$  matrix of the FB coefficients for the SSF block and  $\hat{\mathbf{S}}_{i-1}$  is the estimated block of  $N_F$  symbols in the frequency domain obtained in the previous iteration. Equation (8) can also be written for the n-th symbol in an SSF block as,

$$\bar{X}_{n}^{i} = F_{n}^{i} \tilde{X}_{n} - B_{n}^{i} \hat{X}_{n}^{i-1}, \tag{9}$$

where  $\tilde{X}_n$  is the *n*-th distorted SSF symbol of received block  $\mathbf{Y}$ .

$$\tilde{X}_n = HX_n + \xi_n,\tag{10}$$

and  $\hat{X}_n^{i-1}$  is the n-th estimated SSF symbol in the previous iteration. The equalized SSF symbol in the i-th iteration,  $\bar{X}_n^i$ , is obtained with the help of the coefficients and the estimated SSF symbol that is fed back from the previous iteration. Hence, it is a turbo receiver. The inherent ISI is removed in the

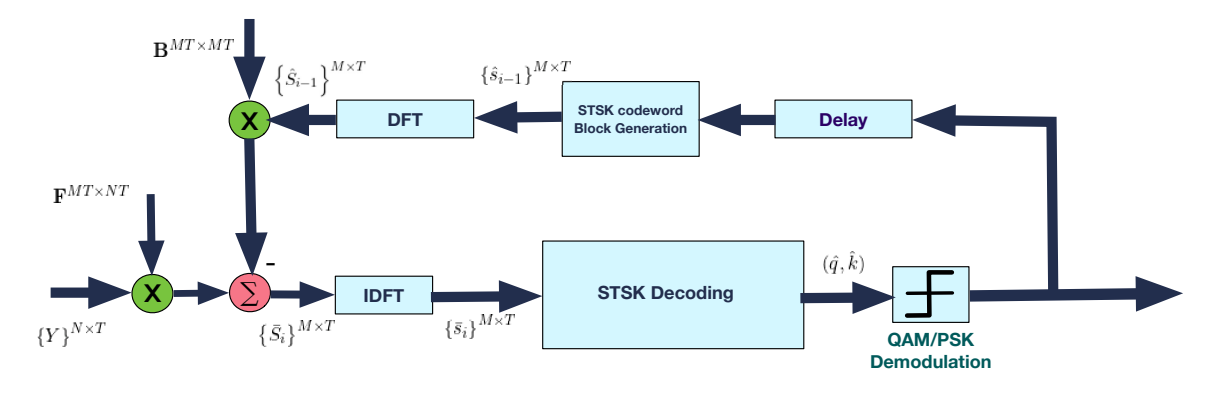


Fig. 4. The proposed iterative space-time block equalizer for STSK-aided single-carrier frequency domain equalization.

frequency domain. The per-symbol mean square error (MSE) at the *i*-th iteration is then given as,

$$MSE^{(i)} = \frac{1}{N_F^2} \sum_{n=1}^{N_F} E\left[ \left| \bar{X}_n^i - X_n \right|^2 \right].$$
 (11)

Once (11) is computed, the signal is converted into the time domain for symbol estimation. Symbol  $\hat{s}_n^i$  is the inverse DFT (IDFT) of  $\hat{X}_n^i$ . The decision block applies vectorial stacking,  $vec(\cdot)$ , on  $\hat{s}_n^i$  for the sake of convenience of the matrix computations involved in the final decision for estimating the DM  $\hat{q}$  and symbol  $\hat{k}$ :

$$(\hat{q}, \hat{k}) = \arg\min_{q,k} \left\| \varphi_n - \kappa_n^{q,k} \right\|^2, \tag{12}$$

where,

$$\varphi_n = vec(\hat{s}_n^i) \in \mathbb{C}^{MT \times 1}, \tag{13}$$

$$\kappa_n^{q,k} = \mathbf{A}\chi_{q,k}^n,\tag{14}$$

and A is the dispersion matrix set given as,

$$\mathbf{A} = [vec(A_1), vec(A_2), \cdots, vec(A_Q)] \in \mathbb{C}^{MT \times Q} \quad (15)$$

$$\chi_{q,k}^n = \left[ \underbrace{0, \cdots, 0}_{q-1}, s_k^n, \underbrace{0, \cdots, 0}_{q-Q} \right]^T \in \mathbb{C}^{Q \times 1}.$$
 (16)

By substituting (9) in (11) we obtain,

$$MSE^{(i)} = \frac{1}{N_F^2} \sum_{n=1}^{N_F} E\left[ \left| (F_n^i \tilde{X}_n^i - B_n^i \hat{X}_n^{i-1}) - X_n \right|^2 \right].$$
(17)

The per-symbol MSE for each iteration depends on the computation of coefficients  $F_n$  and  $B_n$  in the frequency domain. Substituting (9) in (17) we obtain (18) and (19) at the top of the next page. Using (10) we obtain the expected value of  $\tilde{X}_n^i$  as,

$$E\left[\tilde{X}_n^i \tilde{X}_n^{i*}\right] = \sigma_{\tilde{X}}^2 H_n H_n^H + \sigma_{\xi_n}^2 \mathbb{I}_N + \sigma_0^2 \mathbb{I}_N.$$
 (20)

Assuming the non-linear distortion as Guassian, we further simplify (20) as,

$$E\left[\tilde{X}_n^i \tilde{X}_n^{i*}\right] = \sigma_{\tilde{X}}^2 H_n H_n^H + \sigma_e^2 \mathbb{I}_N, \tag{21}$$

where  $\sigma_e^2$  is the effective noise power due to the sum of the nonlinear distortion and the AWGN. The coefficients  $F_n$  and  $B_n$  update iteratively, where the FF filter is responsible for partially equalizing the residual interference and the remainder of it gets equalized by the FB filter. The FB filter coefficient  $B_n^i$  measures the reliability of the reconstructed interference that is subtracted from the partially equalized signal coming from the FF filter.

In order to minimize (17) such that the FB component  $B_n$  cancels out the interference from other symbols in the *i*-th iteration as well as neutralizes the effects of intermodulation distortion  $\xi$ , we define the following constraint [5],

$$\sum_{n=1}^{N_F} B_n^i = 0. (22)$$

We apply the Langrange multipliers method to minimize (17) and obtain,

$$\Psi(F_n^i, B_n^i, \lambda^i) = MSE^{(i)} + \Re\left\{\lambda^i \sum_{n=1}^{N_F} B_n^i\right\}.$$
 (23)

The coefficients of (23) can be found by setting the gradient of  $\Psi(F_n^i, B_n^i, \lambda^i)$  to zero,

$$\nabla_{F^H} \Psi = 0 
\nabla_{B^*} \Psi = 0 
\nabla_{\lambda} \Psi = 0.$$
(24)

The gradients in (24) can be calculated from

$$\begin{array}{c} \bigtriangledown_{F^H} \Psi : F_n^i + F_n^i H_n^H (1 - (\rho^{i-1})^2) H_n \frac{\sigma_X^2}{\sigma_e^2} - H_n^H \frac{\sigma_X^2}{\sigma_e^2} = 0, \\ \bigtriangledown_{B^*} \Psi : F_n^i \cdot H_n - \frac{B_n^i}{\rho^{i-1}} - 1 = 0, \\ \bigtriangledown_{\lambda} \Psi : \sum_{n=1}^{N_F} B_n^i = 0, \end{array}$$

where  $\rho^i$  is the correlation coefficient in the *i*-th iteration. Equation (25) can be further simplified for the *n*-th SSF symbol as,

$$F_n^i = \frac{H_n^H \frac{\sigma_X^2}{\sigma_e^2}}{1 + H_n^H (1 - (\rho^{i-1})^2) H_n \frac{\sigma_X^2}{\sigma_e^2}},$$
 (26)

$$B_n^i = \rho^{i-1} \left( F_n^i \cdot H_n - 1 \right). \tag{27}$$

$$MSE^{i} = \frac{1}{N_{F}^{2}} \sum_{n=1}^{N_{F}} \left( E\left[\bar{X}_{n}^{i} \bar{X}_{n}^{iH}\right] + \sigma_{X_{n}}^{2} - 2\Re\left\{ E\left[\bar{X}_{n}^{iH} X_{n}\right]\right\} \right). \tag{18}$$

$$E\left[\bar{X}_{n}^{i}\bar{X}_{n}^{iH}\right] = F_{n}^{i}E\left[\tilde{X}_{n}^{i}\tilde{X}_{n}^{i*}\right]F_{n}^{iH} + \left|B_{n}^{i}\right|^{2}\sigma_{\hat{X}_{n}^{i}}^{2} - 2\Re\left\{B_{n}^{i*}F_{n}^{i}H_{n}E\left[\tilde{X}_{n}^{i}\hat{X}_{n}^{i-1*}\right]\right\}$$
(19)

TABLE I SIMULATION PARAMETERS.

Parameters	Value
Sampling Frequency	5 MSamples/s
Bandwidth	5 MHz
Blocker Modulation	BPSK
Blockers Power (dB)	-52 & -62
Roll-off factor, $\beta$	0.20
STSK configuration $(M, N, T, Q)$	(2,2,2,Q) & (4,4,2,Q)
Dispersion Matrix, Q	2, 4
Modulation Order	QPSK
Channel Model	Extended Vehicular Channel - A
Block Size	512
Iterations $N_I$ for ISTBE	4
CP length	16

For QPSK systems, the correlation coefficient  $\rho^i$  can also be obtained using the estimated SNR  $\hat{\gamma}^i$  at the output of demodulation process,

$$\rho^i = 1 - 2P_b^i, (28)$$

where the error probability is,

$$P_b^i = Q\left(\sqrt{\hat{\gamma}^i}\right),\tag{29}$$

and  $Q(u)=\frac{1}{2\pi}\int_u^\infty e^{t^2/2}dt$ . Together with hard decision estimates, the correlation coefficient reduces the error propagation and, hence, helps with the convergence. The correlation coefficient is calculated based on the assumption that the additional noise resulting from the intermodulation distortion at the output of the equalizer is Gaussian distributed. Moreover, the residual ISI can also be approximated by a Gaussian distribution from the central-limit theorem.

It is worth noting that the STSK encoder is added in the FB chain, as shown in Fig. 4, in order to reconstruct the interference and remove it iteratively from the received signal. The interference arises as a result of the inherent ISI and the intermodulation term (7). This is stated mathematically in (8).

Table II presents the computational complexity of the proposed receiver along with the complexity of the SSF-MMSE receiver as a reference. The complexity of the ISTBE receiver is mainly driven by the FB and FF filters together with the operations performed for the reconstruction of the feedback signal. This complexity is only slightly higher than that of the MMSE receiver, but it is practically affordable with available processing technology.

### V. SIMULATION RESULTS

The simulations are performed in MATLAB with the parameters specified in Table I. The derived DM sets are valid for

QPSK only. For higher order modulations (16QAM, 64QAM, etc.) and higher MIMO orders, the derivation of the DM needs to be reformulated. The performance of the proposed SSF-ISTBE is compared against the state-of-the-art SSF-MMSE [10] in the presence of receiver nonlinearity. We assume that the channel coherence time is shorter than the STSK codeword duration

We consider  $IIP_3=-20~\mathrm{dBm}$  which corresponds to  $\alpha_3=1.333\times 10^3~\mathrm{for}~\alpha_1=1$  [12]. Such low  $IIP_3$  characterizes a receiver of poor nonlinear characteristics. The total noise power is set to  $-107~\mathrm{dBW}$  for the operating bandwidth. The spectral efficiency can be obtained from,

$$\varrho = \frac{\log_2(Q \cdot K)}{T(1+\beta)} \quad [bps/Hz]. \tag{30}$$

Fig. 5 shows that the proposed framework achieves near optimal performance and significantly improved performance with respect to the corresponding MMSE receiver for blocker powers of B=C=-62 dBW. The SSF-ISTBE achieves a gain of approximately 4 dB in the high SNR regime over the MMSE receiver. Such resilience is because of the spacetime diversity in addition to the iterative process of the ISTBE which suppresses the intermodulation distortion as a result of the multiplicative effects of nonlinearity at the output of the equalization process. Increasing the blocker power to B = C = -52 dBW introduces an overwhelming nonlinear distortion and the gain diminishes as seen in Fig. 5. The BER curve slope at the signal-to-blocker power ratio (SBR) of -30 dB at  $E_b/N_0 = 25 \text{ dB}$  for B = C = -52 dBWin Fig. 5 indicates that the STSK configuration (2,2,2,2) can withstand very strong blockers, as long as the  $SBR \ge -30$ dB.

Increasing the STSK MIMO order to (4,4,2,4), also increases the multiplicative effects of nonlinearity and the performance is noticeably improved over the MMSE and a maximum gain of 6 dB is observed for moderate blocker powers. The BER curve inflection point characterized by the SBR of  $-35~{\rm dB}$  at  $E_b/N_o=20~{\rm dB}$  for  $B=C=-52~{\rm dBW}$  shows the immunity of the (4,4,2,4) configuration even for such a low SBR, specifically for the SSF-ISTBE. The higher MIMO order increases the resilience of the SSF-ISTBE against receiver nonlinearity.

### VI. CONCLUSION

This paper has introduced an efficient iterative receiver for practical STSK single-carrier communications systems. We have evaluated its performance for nonlinear RF receiver front ends. The BER results provide two important insights: The

### TABLE II COMPUTATIONAL COMPLEXITY.

Receiver	Computational Complexity
SSF-MMSE	$\frac{4M^2N + 8MN + 4MTQ + 2QK' + Q + 2K}{\log 2(Q \cdot K)}$
SSF-ISTBE	$\frac{N_I \left(4MN(M+2) + 4MTQ + Q + 2QK' + 2K + N_F \log_2(N_F) + N_F MT\right)}{\log 2(Q \cdot K)}$

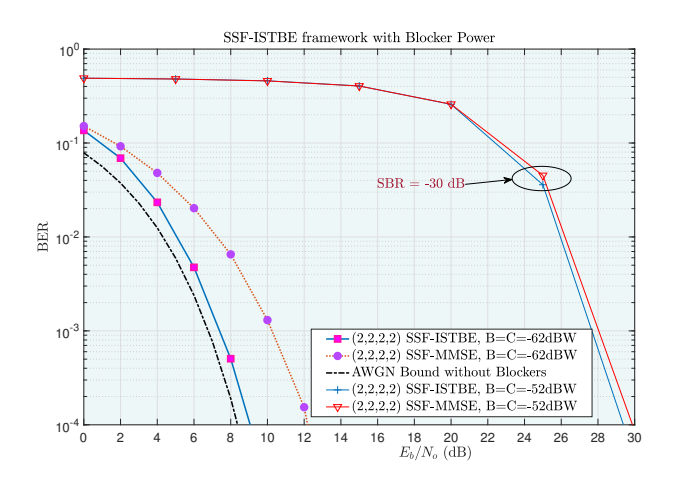


Fig. 5. Performance comparison of the (2,2,2,2)-QPSK configuration between the proposed SSF-ISTBE framework and the SSF-MMSE. This configuration offers a spectral efficiency of  $\varrho=1.25$  bps/Hz.

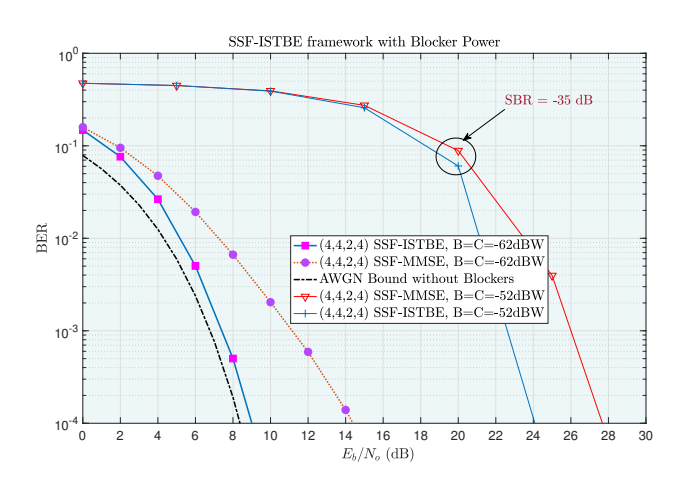


Fig. 6. Performance comparison between the proposed SSF-ISTBE and the SSF-MMSE receivers for the (4,4,2,4)-QPSK configuration. This configuration offers a spectral efficiency of  $\varrho=1.66$  bps/Hz.

proposed SSF-ISTBE has a significant gain over the SSF-MMSE and this gain increases with the number of antennas. The SSF is resilient to strong blockers that cause in-band intermodulation distortion in practical receivers. Our numerical results have shown that there is no performance degradation for poor RF front ends when the blockers are 45 dB above the noise floor. When both blockers are 55 dB above the noise power, the receiver is able to demodulate the desired signals

when the SBR is as low as -30 and -35 dB for for a two and four-antenna systems, respectively, without any additional processing. In practice this enables considering SSF-ISTBE without having to rely on tight RF filters and expensive RF front end components, but rather provide frequency agility through wide channel selection filters and simple RF front ends. This is specifically useful for the IoT and for radios operating in shared spectrum where heterogeneous signals will need to coexist and the neighboring transmitters, their locations, the transmit powers, and transmit patterns are unknown.

### ACKNOWLEDGMENT

This work is supported in part by the National Science Foundation under grant numbers CNS-1564148 and ECCS-2030291.

#### REFERENCES

- F. Tariq, M. R. Khandaker, K.-K. Wong, M. A. Imran, M. Bennis, and M. Debbah, "A speculative study on 6G," *IEEE Wireless Communications*, vol. 27, no. 4, pp. 118–125, 2020.
- [2] L. Zhang, Y.-C. Liang, and M. Xiao, "Spectrum sharing for Internet of Things: A survey," *IEEE Wireless Communications*, vol. 26, no. 3, pp. 132–139, 2018.
- [3] T. F. Rahman, V. Pilloni, and L. Atzori, "Application task allocation in cognitive IoT: A reward-driven game theoretical approach," *IEEE Transactions on Wireless Communications*, vol. 18, no. 12, pp. 5571–5583, 2019.
- [4] H. Yan and H. Yang, "Pilot length and channel estimation for massive MIMO IoT systems," *IEEE Transactions on Vehicular Technology*, vol. 69, no. 12, pp. 15 532–15 544, 2020.
- [5] T. F. Rahman, V. Marojevic, and C. Sacchi, "Iterative equalization of STSK-aided single-carrier systems: Design and analysis with non-ideal power amplifiers," *IEEE Transactions on Vehicular Technology*, pp. 1– 11, 2021.
- [6] S. Sugiura, S. Chen, and L. Hanzo, "Coherent and differential spacetime shift keying: A dispersion matrix approach," *IEEE Transactions on Communications*, vol. 58, no. 11, pp. 3219–3230, 2010.
- [7] M. I. Kadir, S. Sugiura, S. Chen, and L. Hanzo, "Unified MIMO-multicarrier designs: A space-time shift keying approach," *IEEE Communications Surveys & Tutorials*, vol. 17, no. 2, pp. 550–579, 2014.
- [8] Y. Zhao, P. Yang, Y. Xiao, L. Xiao, B. Dong, and W. Xiang, "An improved frequency domain turbo equalizer for single-carrier spatial modulation systems," *IEEE Transactions on Vehicular Technology*, vol. 66, no. 8, pp. 7568–7572, 2017.
- [9] L. Xiao, Y. Xiao, Y. Zhao, P. Yang, M. Di Renzo, S. Li, and W. Xiang, "Time-domain turbo equalization for single-carrier generalized spatial modulation," *IEEE Transactions on Wireless Communications*, vol. 16, no. 9, pp. 5702–5716, 2017.
- [10] T. F. Rahman, A. Habib, C. Sacchi, and M. El-Hajjar, "Mm-wave STSK-aided single carrier block transmission for broadband networking," in 2017 IEEE Symposium on Computers and Communications (ISCC). IEEE, 2017, pp. 507–514.
- [11] E. Rebeiz, A. S. H. Ghadam, M. Valkama, and D. Cabric, "Spectrum sensing under RF non-linearities: Performance analysis and DSP-enhanced receivers," *IEEE Transactions on Signal Processing*, vol. 63, no. 8, pp. 1950–1964, 2015.
- [12] J. Dsouza, H. Mohammadi, A. V. Padaki, V. Marojevic, and J. H. Reed, "Symbol error rate with receiver nonlinearity," in 2020 IEEE 91st Vehicular Technology Conference (VTC2020-Spring), 2020, pp. 1–5.
- [13] Q. Zou, M. Mikhemar, and A. H. Sayed, "Digital compensation of cross-modulation distortion in software-defined radios," *IEEE Journal* of Selected Topics in Signal Processing, vol. 3, no. 3, pp. 348–361, 2009
- [14] T. F. Rahman and C. Sacchi, "A low-complexity linear receiver for multiuser MIMO SC-FDMA systems," in 2016 IEEE Aerospace Conference, 2016, pp. 1–6.